A Robust Ultra-Broad-Band Wireless Communication System Using SAW Chirped Delay Lines

Andreas Springer, *Associate Member, IEEE,* Mario Huemer, *Student Member, IEEE,* Leonhard Reindl, *Member, IEEE,* Clemens C. W. Ruppel, *Senior Member, IEEE,* Alfred Pohl, *Member, IEEE,* Franz Seifert, *Senior Member, IEEE,* Wolfgang Gugler, *Student Member, IEEE,* and Robert Weigel, *Senior Member, IEEE*

***Abstract*—Design and performance of a low-cost wireless communication system for indoor and industrial environments are presented. The system is based on chirp-signal transmission to achieve a robust communication link. For the chirp expansion and compression, surface acoustic wave chirped delay lines fabricated from $LiTaO_3$-X112rotY are used. Center frequency, bandwidth, and chirp rate are 348.8 MHz, 80 MHz, and $\pm$40 MHz/μs, respectively. An optimized square-root weighting was chosen to reduce the sidelobes of the compressed pulse to -42 dB compared to the correlation peak. The chirp filters have been deployed in a hardware demonstrator for data rates of up to 5 Mb/s. Limiting factors for the data rate according to simulations and measurements are mainly intersymbol interferences due to the time overlapping of consecutive symbols and, to a lower extent, the multipath propagation.**

***Index Terms*—Chirp signals, spread spectrum communication, surface acoustic waves, wireless communications.**

I. Introduction

THE wireless communications market has undergone a tremendous growth. This is mainly due to the rapidly expanding area of personal communication services (PCS's) like cellular or cordless phone systems, paging and wireless local area networks (WLAN's). Some applications like cellular phone systems are already widely accepted, although market penetration is still far from saturation, while others, e.g., WLAN's, are just starting to become a common technology [1]. Driven by the rapid development of RF technologies for PCS's, wireless communication systems for industrial environments are now facing strong interest. Here, major applications are flexible and mobile data-transmission links between sensors, actuators, autonomous vehicles, robots, and controller units. Due to the hostile electromagnetic environment, which includes severe electromagnetic emissions from other devices as well as heavy distortions due to multipath propagation, the robustness of the communication link is extremely important.

Manuscript received March 24, 1998; revised August 27, 1998.

A. Springer, M. Huemer, W. Gugler and R. Weigel are with the Institute for Communications and Information Engineering, University of Linz, A-4040 Linz, Austria.

L. Reindl and C. C. W. Ruppel are with Siemens AG Munich, Research and Development Center, D-81739 Munich, Germany.

A. Pohl and F. Seifert are with the Applied Electronics Laboratory, University of Technology Vienna, A-1040 Vienna, Austria.

Publisher Item Identifier S 0018-9480(98)09218-7.

The spread-spectrum technology is especially well suited to provide such a robust data transmission even in very noisy radio environments [2]. Originally developed for military purposes, spread-spectrum communication is currently a popular technology in many areas of mobile communications. It is established in the IS-95 standard for cellular phones, as well as in the IEEE 802.11 standard for WLAN's [1] and, very recently, it has been chosen to be part of the third-generation cellular phone system standard UMTS. Key features of the spread-spectrum technology are high immunity against multipath phenomena, high spectral efficiency, low power, and low cost. The critical operations in spread-spectrum systems are the spreading and despreading functions in the transmitter and receiver, respectively. The common system concepts [direct-sequence (DS) and frequency hopping (FH)] require rather sophisticated circuit designs and system realizations to accomplish the despreading in the receiver. In particular, the synchronization of the despreading code sequence is a difficult task. With the well-known FM chirp signals and the associated technique of pulse compression with its high processing gain, which is widely used in radar systems [3], another kind of spread-spectrum communication system can be realized [4]. In such a system, the spectrum spreading is used for combating the multipath distortions, whereas code-division multiple access (CDMA) can only be realized if additional coding is introduced [5].

The generation of the transmitted chirp signals and the correlation process in the receiver are vital to the chirp system. Both functions are easily accomplished by using surface acoustic wave (SAW) chirped delay lines [3], which are well suited for use as expansion and compression filter in the proposed communication system due to their high degree of flexibility in designing desired transfer functions. SAW chirped delay lines can be realized at small size and low cost, as is the case with the well-established SAW filters and resonators in wireless communication products [6], [7]. Our system, which is designed for unlicensed use in indoor and industrial environments in the ISM band at 2.45 GHz, uses binary orthogonal keying (BOK) as modulation scheme by making use of the quasi-orthogonality of up- and down-chirp signals, which leads to a very robust communication link. In the following, we give a short description of the proposed system and its parameters, design and fabrication of the SAW chirped delay lines are described, radio channel simulation and measurement, an issue of great relevance to every wireless communication system, is covered, and results of the system simulation, as well as measurement results achieved with a hardware demonstrator, are given.

II. System Overview

A. Basic Chirp Theory

A chirp waveform can be written as

$$s(t) = a(t)\cos[\Theta(t)] \tag{1}$$

where $\Theta(t)$ is the time-domain phase, and $a(t)$ is the time-domain envelope, which is zero outside a time interval of length T. The instantaneous frequency is defined as

$$f_M(t) = \frac{1}{2\pi}\,\frac{d\Theta(t)}{dt}. \tag{2}$$

The rate of change of the instantaneous frequency

$$\mu(t) = \frac{df_M(t)}{dt} = \frac{1}{2\pi}\,\frac{d^2\Theta(t)}{dt^2} \tag{3}$$

is denoted the chirp rate. Waveforms with $\mu(t) > 0$ are called up-chirps while those with $\mu(t) < 0$ are called down-chirps. For a linear chirp, $\mu(t)$ is constant and, hence, $f_M(t)$ is a linear function of t, and $\Theta(t)$ is a quadratic function. If we take the waveform $s(t)$ to be centered at $t = 0$, it can be written as

$$s(t) = a(t)\cos[2\pi f_0 t + \pi\mu t^2 + \varphi_0] \tag{4}$$

where f_0 is the center frequency, φ_0 is the phase constant, and $a(t) = 0$ for $|t| > T/2$. It is convenient to define the chirp bandwidth B as the range of instantaneous frequencies so that

$$B = |\mu| T. \tag{5}$$

The 3-dB bandwidth of the spectrum is dependent on the shape of $a(t)$ and can be different from B.

If a chirp waveform is fed into its matched filter whose impulse response is also a chirp waveform, but with its frequency varying in the opposite direction, then the output signal typically has a narrow RF peak at the chirp center frequency. Generally, the width of the output peak is much less than the length T of the input waveform and, hence, the process is called pulse compression, and the matched filter is commonly named compressor. If we regard chirp waveforms with flat envelopes and if we take the matched filter also to be centered at $t = 0$, e.g.,

$$h(t) \sim s(-t) \tag{6}$$

then we can find an analytical expression for the output waveform $g(t)$ of the matched filter. We have

$$g(t) = h(t) * s(t) = \varphi_{ss}(t) \tag{7}$$

where $\varphi_{ss}(t)$ is the autocorrelation function of $s(t)$. It can be shown [8] that $\varphi_{ss}(t)$ is given by

$$\varphi_{ss}(t) = \sqrt{BT}\,\frac{\sin\left\{\pi Bt\left(1 - \dfrac{|t|}{T}\right)\right\}}{\pi Bt}\cos(2\pi f_0 t) \tag{8}$$

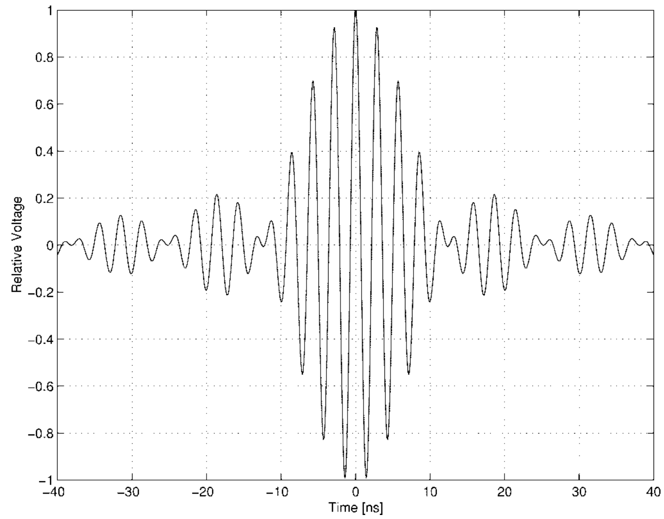

Fig. 1. Autocorrelation function for a linear chirp signal with the parameters $T = 2\,\mu$s, $B = 80$ MHz, and $f_c = 348.8$ MHz.

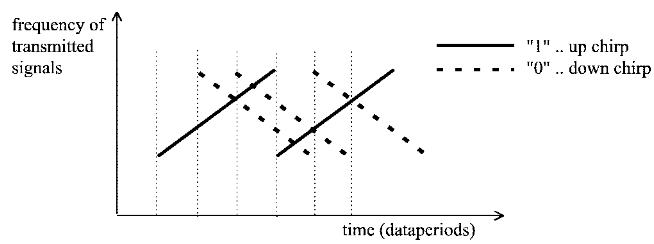

Fig. 2. Schematic of a SAW BOK wireless local area network (LAN).

for $-T < t < T$. This is illustrated in Fig. 1 for the parameters $T = 2\,\mu$s, $B = 80$ MHz, and $f_c = 348.8$ MHz, which are used in our proposed system. The envelope has its maximum at $t = 0$, and its first zeros at $t \approx \pm 1/B$. It is convenient to specify the pulsewidth as $1/B$. This gives a value of 12.5 ns for the given example. The ratio of the input and output pulsewidths is given by the time-bandwidth product TB, which is known as compression ratio or processing gain. Another important parameter is the sidelobe rejection, which here is about 13 dB. A common method of reducing the sidelobes is to apply amplitude weighting of the chirp signal, which is described in more detail in Section III.

B. BOK

Fig. 2 shows the principle of the BOK modulation scheme in the time-frequency plane. If we send a “high,” an IF pulse at the chirp center frequency of 348.8 MHz stimulates the up-chirp filter, if we send a “low,” the down-chirp filter is stimulated. With a chirp-signal duration of $2\,\mu$s the highest achievable data rate would be only 500 kb/s, which is too low for today’s systems. To increase the data rate, the chirp signals have to overlap in time, as is shown in Fig. 2. By that measure, the data rate of our system is 2 Mb/s. The sum of both filter outputs is launched at a transmitter frequency of 2.45 GHz. In the receiver, the signal, which is disturbed by the frequency-selective radio channel and additive noise, is mixed down and fed into the SAW compressor filters. The up-chirp filter is matched to the “low” signal, the down-chirp

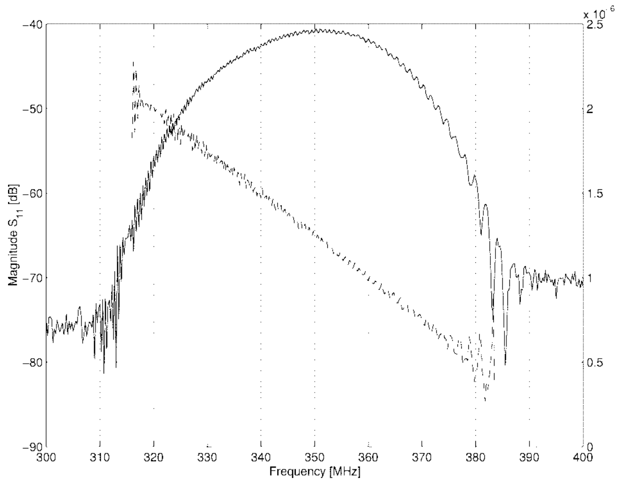

Fig. 3. Measured transfer function and group delay of an optimized square-root weighted down-chirp filter.

filter to the "high" signal. In both paths, noncoherent envelope detection with hard decision and an adaptive threshold control follows. The schematic of the system is presented in Fig. 10 in Section VI, together with a more detailed description of the realized system.

The effect of overlapping and the fact that up- and down-chirps are not exactly orthogonal leads to disturbing cross correlations in both filter outputs. This limits the achievable data rate because the cross-correlation peaks grow together with the overlapping of consecutive chirp signals in time. The ultimative limit for the data rate is given by the time spreading of the correlation peaks caused by the multipath channel.

III. SAW Chirped Delay Lines

Up- and down-chirp filters have been designed and fabricated from $LiTaO_3$-X112rotY substrate using a standard optical lithography technique. As metallization a layer of 72-nm aluminum has been deployed. The filters have a center frequency and bandwidth of 348.8 and 80 MHz, respectively. According to [9], two apodized transducers were used and a split-finger arrangement was chosen to avoid internal reflections. The chip size is 11.8×2.0 mm^2. An optimized square-root weighting of the magnitude of the filter transfer function was employed to reduce the sidelobes of the compressed pulse to -42 dB compared to the correlation peak. Measurement results of the transfer function and group delay of a down-chirp filter are shown in Fig. 3. The chirp rate of the filters is about ± 40 MHz/μs, which results in a dispersion time of about 2 μs. This corresponds to a time-bandwidth product of 22 dB.

IV. Radio-Channel Measurements and Simulations

To improve the performance of a communication system in a timely, cost-effective, and effort-free manner, it is necessary to use computer-aided analysis. The computational model for the indoor radio channel is crucial to the reliability of the simulation results for our proposed system. To collect data concerning the properties of the indoor radio channel, wide-band measurements [10], [11] at 2.45 GHz have been conducted for line-of-sight (LOS) and non-line-of-sight (NLOS) scenarios in a laboratory/office environment in the fourth floor of a six-story building. From the measured impulse response profiles, mean delay spread, coherence bandwidth, and path-loss exponents have been derived. Comparison with simulation results extracted from the SIRCIM simulator [12]—a tool for modeling indoor radio channels—has also been made.

A. Parameters of the Indoor Radio Channel

The baseband complex-channel impulse response of the indoor radio channel is modeled as [13]

$$h(t) = \sum_{k=0}^{N-1} a_k e^{j\Theta_k} \delta(t - \tau_k). \tag{9}$$

Here, k is the path index, a_k the path gain, Θ_k the phase shift, and τ_k the time delay of the kth path. The absolute delay of the channel is not important, so τ_0 is set to zero. The root-mean-square (rms) delay spread, which is a measure for the time-dispersion of a transmitted signal, is defined as

$$\tau_{\rm rms} = \sqrt{\frac{\int_{-\infty}^{\infty} (t - \tau_m)^2 |h(t)|^2 \, dt}{\int_{-\infty}^{\infty} |h(t)|^2 \, dt}} \tag{10}$$

where τ_m is the mean excess delay given by

$$\tau_m = \frac{\int_{-\infty}^{\infty} t |h(t)|^2 \, dt}{\int_{-\infty}^{\infty} |h(t)|^2 \, dt}. \tag{11}$$

We use a simple path-loss model of the form d^n where d is the distance between the transmitter and the receiver, and n indicates the path-loss exponent. The mean path loss in decibels is described as [14]

$$\overline{PL}(d) = \overline{PL}(d_0) + 10n \log_{10}\left(\frac{d}{d_0}\right) \tag{12}$$

where free-space path loss is assumed between the transmitter and a reference distance d_0, so that $\overline{PL}(d_0)$ is given by

$$\overline{PL}(d_0) = 20 \log_{10}\left(\frac{4\pi d}{\lambda}\right) - G_T - G_R \tag{13}$$

where λ is the wavelength, and G_T and G_R are the antenna gains in decibels.

B. Measurement Setup

The measurement technique applied here is a wide-band coherent frequency-response measurement, where magnitude and phase shift at 1601 equidistant frequency points in the selected frequency band (2.4–2.5 GHz) are recorded. The measurement setup is shown in Fig. 4. The system consists of

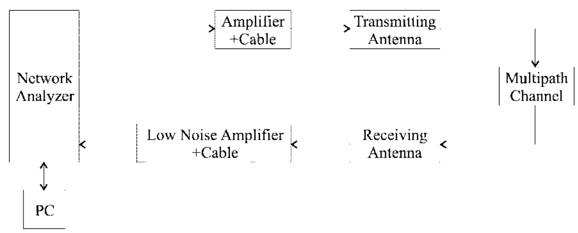

Fig. 4. Setup for radio-channel measurement.

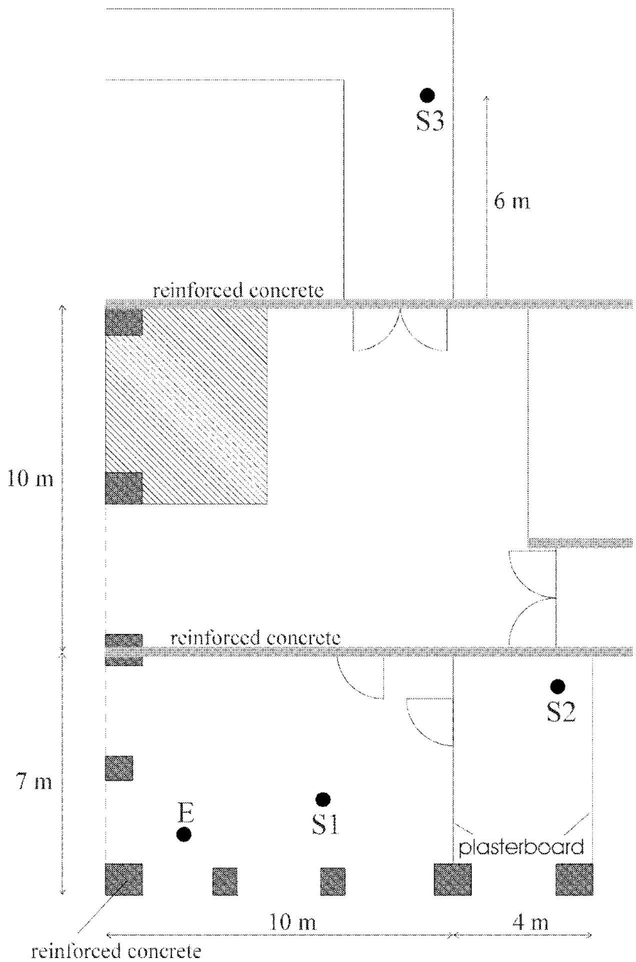

Fig. 5. Environment for radio-channel measurement.

an HP 8753 network analyzer, two broad-band ground plane antennas with a gain of 2 dBi, and a low-noise amplifier.

Before the measurements are carried out, the system has to be calibrated at the frequency band of interest in order to compensate for the influence of phase and amplitude variations imposed by the cables, amplifiers, and other measurement equipment.

C. Measurement Environment

The measurements have been performed in a laboratory/office environment in the fourth floor of a six-story building. We used three types of locations ($S1$: laboratory room, $S2$: office room, $S3$: hallway) for our measurements, as is shown in Fig. 5. The tests have been done at 19 discrete locations separated by $\lambda/4$ along a 4.5 λ-track at each of the three positions marked with $S1$, $S2$, and $S3$, as well as at different positions in all rooms to achieve enough data for a delay spread and a path-loss estimation. During the measurements, we kept the channel as time invariant as possible.

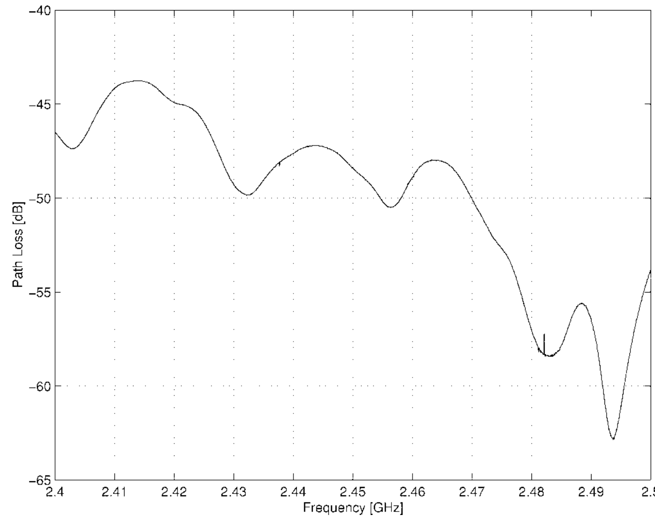

Fig. 6. Frequency response of the radio channel for transmitter position $S1$ in the laboratory room.

TABLE I
COMPARISON OF MEASURED AND SIMULATED PATH-LOSS EXPONENTS

Topography	n measured	n simulated
LOS	2.1	2.3
NLOS	2.7	2.9

D. Measurement and Simulation Results

Measured impulse response results have been compared with results produced with the SIRCIM simulator.[1] SIRCIM is a microwave multipath indoor radio-channel simulator designed from propagation measurements made in over ten different buildings. The simulator allows the choice of the carrier frequency, building type, topography, velocity of the mobile receiver, and transmitter–receiver separation. After the parameters are chosen, the simulator produces multipath-power delay profiles at $\lambda/4$ separations along 4.5 λ-tracks.

Fig. 6 shows the frequency response of the channel for the transmitter position $S1$ in the laboratory room. The path loss has been computed as the average power loss over the measured frequency band. The path-loss exponent has been determined separately for LOS and NLOS topographies. In both cases, the path loss $\overline{PL}(d)$ in decibels has been drawn as a function of the logarithm of d/d_0. From the results, the path-loss exponent n has been determined by fitting a regression line through the measured points. Table I compares experimental and computed results.

Fig. 7 compares measured and simulated impulse response profiles for a transmitter–receiver distance of 5 m and LOS topography ($S1$). Table II shows measured and simulated estimates for the rms delay spread. Measurements and simulations indicate that the mean delay spread is significantly larger in

[1] D. M. Krizman, B. J. Ellison, and T. S. Rappaport, *SIRCIM Plus: Simulation of Indoor Radio Channel Impulse Response Models with Impulse Noise*, Rev 1.0, Dec. 1996.

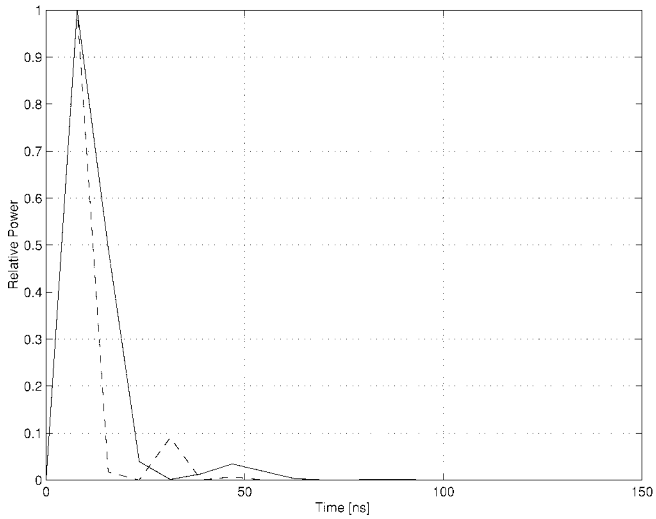

Fig. 7. Comparison between measured (solid line) and simulated (dashed line) indoor channel impulse responses for a transmitter receiver separation of 5 m and LOS topography.

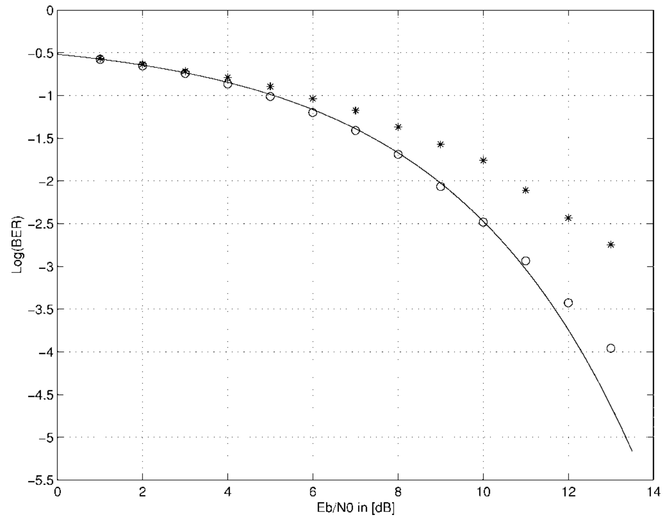

Fig. 8. BER versus E_b/N_0 for orthogonal signals. Theoretical limit after [15] (solid line), nonoverlapping 2-μs-long chirp signals (-∘-), and overlapping 2-μs-long chirp signals with a data rate of 2 Mb/s (-∗-).

TABLE II
COMPARISON OF MEASURED AND SIMULATED ESTIMATES FOR THE rms DELAY SPREAD

Location	T–R separation [m]	$\overline{\tau_{rms}}$ [ns] measured	$\overline{\tau_{rms}}$ [ns] simulated
$S1$ (LOS)	5	12.8	14.1
$S2$ (NLOS)	12	37.9	36.6
$S3$ (NLOS)	22	48.2	34.7

NLOS topographies. Summarizing, we can say that experimental and computed data coincide well so that the SIRCIM simulator can be used as a basis for realistic simulations of indoor wireless systems.

V. Simulation Results

Simulations have been carried out to evaluate the performance of the proposed chirp spread-spectrum system. MATLAB software has been used for the simulation and all computations have been carried out in baseband. Both the chirp filters and radio-channel model have been implemented as discrete frequency transfer functions. The effect of the multipath fading radio channel has been modeled with the simulation software SIRCIM, as is described in Section IV. In the receiver, an envelope detector followed by a decision device with a fixed threshold has been implemented and ideal symbol timing and clock recovery have been assumed.

For the ideal case of an additive white Gaussian noise (AWGN) channel, the effect of the time overlapping of consecutive chirp signals is plotted in Fig. 8 in terms of bit error rate (BER) versus the signal-to-noise-ratio E_b/N_0, which is the ratio of the average bit energy to the noise power density. The solid line represents the theoretical result for fully orthogonal signals [15]. The result for nonoverlapping 2-μs-long chirp signals (at a data rate of 500 kb/s, -∘- curve) almost approaches the theoretical limit. The chirp system is slightly worse only for high values of E_b/N_0 due to the fact that up- and down chirps are not exactly orthogonal. Thus, if an up-chirp signal is

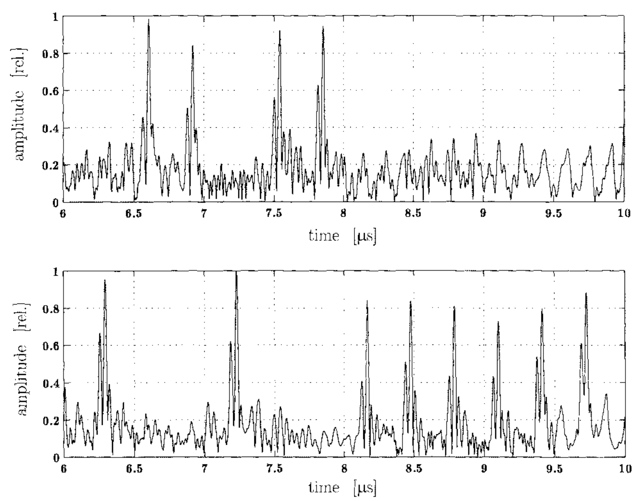

Fig. 9. Simulated output of the receiver chirp filters after envelope detection.

compressed in an up-chirp filter (which is the matched filter for a down-chirp signal), a small cross-correlation peak appears at the filter output. This can be seen in Fig. 9 where the output of the receiver chirp filters after envelope detection is depicted. The occurring intersymbol interference (ISI) between up- and down-chirp grows as the overlapping of consecutive chirps increases, which is demonstrated in Fig. 8 for a data rate of 4 Mb/s with 2-μs-long chirp signals (-∗- curve). Here, the deviation from the theoretical limit starts already at values of E_b/N_0 as low as 4 dB.

The ISI between up- and down-chirp mainly limits the actual data rate. The time dispersion due to the multipath fading channel also causes distortions in the receiver signal. As shown in Fig. 9, these multipath distortions are represented by multiple pulses in the compressed signal. Delay spreads in an indoor environment at UHF frequencies are typical below 50 ns. Therefore, these distortions do not contribute significantly to the BER compared to the cross-correlation between up- and down-chirp. As can be seen in Fig. 9, the distortions due to

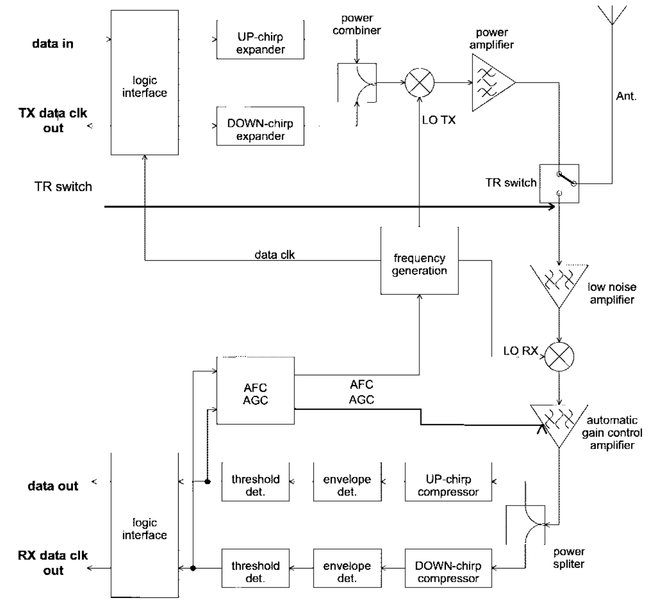

Fig. 10. Schematic of the hardware demonstrator.

ISI are increasing if several consecutive chirps of one kind are transmitted. This case must be prevented by using proper source coding.

VI. Experimental Results

A hardware demonstrator has been set up to prove the feasibility of the proposed system as well as to demonstrate its robustness for wireless indoor data communications. The schematic of the demonstrator is depicted in Fig. 10. After combining the two quasi-orthogonal chirp signals, the IF signal is up-converted to the 2.45-GHz band. The transmitted power was +13 dBm. We used time-duplex operation for the system. A transmit/receive switch isolates the transmitter from the receiver path. A low-noise amplifier combined with a bandpass filter in the receiver path is followed by a mixer and an automatic gain control amplifier. The down-converted signal is fed into the matched dispersive SAW delay lines, by which the signal is compressed in time, thus enhancing the amplitude for sampling. After a simple, but reliable envelope detector, the signal is processed by an adaptive threshold decision device followed by the interface logic as well as automatic frequency and automatic gain control circuits. The output of the receiver filter after envelope detection for a data rate of about 3.2 Mb/s is shown in Fig. 11. There is a good qualitative agreement between the measured and simulated output signals of the chirp filters in the receiver after envelope detection. The slightly higher noise in the measured result can be attributed to the transmitter and receiver electronics, which has been modeled ideally for the simulation. Both stimulations and measurements indicate that for data rates of a few megabits per second and for typical delay spreads in indoor environments, the simple threshold device in the receiver can be used. For higher data rates, more elaborate receiver structures like time-windowing receivers, Rake receivers or higher order modulation receivers have to be used and the weighting of the chirp filters should be

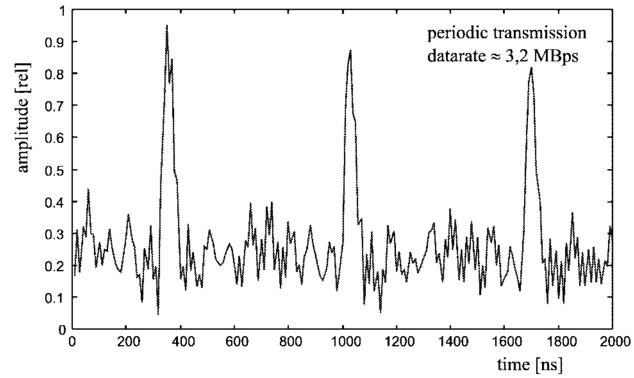

Fig. 11. Measured output of the receiver up-chirp compressor after envelope detection.

optimized regarding pulse energy, sidelobe suppression, and cross correlation.

VII. Conclusion

We have presented performance results of a low-cost wireless communication system based on SAW chirped delay lines fabricated on $LiTaO_3$-X112rotY. The system uses BOK as a modulation scheme to provide both a robust and low-cost solution. Simulations show that our system almost attains the theoretical BER limit for the AWGN case. For use in indoor and industrial environments with their strong multipath fading distortions as well as severe electromagnetic emissions from other devices, our results, which were derived from simulations and measurements made with a hardware demonstrator, indicate that the system performs well up to bit rates of 5 Mb/s which easily covers many commercial applications such as e.g., wireless Internet access. The achievable data rate is limited by the chirp-signal duration and chirp-signal overlapping, respectively. For higher data rates, more refined transmission techniques and more complex receiver structures have to be implemented.

Acknowledgment

The authors would like to acknowledge the many fruitful discussions with R. Bächtiger, M. Loder, and H. Küpfer, Siemens Schweiz AG, Zürich, Switzerland.

References

[1] B. P. Crow, I. Widjaja, J. G. Kim, and P. T. Sakai, "IEEE 802.11 wireless local area networks," *IEEE Commun. Magazine.*, vol. 35, no. 9, pp. 116–126, Sept. 1997.

[2] R. C. Dixon, *Spread Spectrum Systems with Commercial Applications*. New York: Wiley, 1994.

[3] D. P. Morgan, *Surface-Wave Devices for Signal Processing*, 2nd ed. Amsterdam, The Netherlands: Elsevier, 1991.

[4] W. Hirt and S. Pasupathy, "Continuous phase chirp (CPC) signals for binary data communication—Part I: Coherent detection and Part II: Noncoherent detection," *IEEE Trans. Commun.*, vol. COM-29, pp. 836–858, June 1981.

[5] M. Kowatsch and J. T. Lafferl, "A spread-spectrum concept combining chirp modulation and pseudonoise coding," *IEEE Trans. Commun.*, vol. COM-31, pp. 1133–1142, Oct. 1983.

[6] D. Penunuri, "Recent progress in SAW filters at GHz frequencies," in *IEEE MTT-S Int. Microwave Symp. Dig.*, vol. I, 1997, pp. 169–172.

[7] M. Hikita, N. Shibagaki, A. Isobe, K. Asai, and K. Sakiyama, "Recent and future RF SAW technology for mobile communications," in *IEEE MTT-S Int. Microwave Symp. Dig.*, vol. I, 1997, pp. 173–176.

[8] C. E. Cook and M. Bernfeld, *Radar Signals—An Introduction to Theory and Application*. New York: Academic, 1967.

[9] C. C. W. Ruppel, L. Reindl, and K. Wagner, "Optimum design of low time-bandwidth product SAW filters," in *Proc. IEEE Ultrason. Symp.*, 1994, pp. 61–65.

[10] M. Huemer, A. Pohl, W. Gugler, A. Springer, R. Weigel, and F. Seifert, "Design and verification of a SAW based chirp spread spectrum system," in *IEEE MTT-S Int. Microwave Symp. Dig.*, vol. I, 1998, pp. 189–192.

[11] N. Papadakis, A. Hatziefremidis, A. Tserolas, and P. Constantinou, "Wideband propagation measurements and modeling in indoor environment," *Int. J. Wireless Info. Networks*, vol. 4, no. 2, pp. 101–111, 1997.

[12] T. S. Rappaport, S. Y. Seidel, and K. Takamizawa, "Statistical channel impulse response models for factory and open plan building radio communication system design," *IEEE Trans. Commun.*, vol. 39, pp. 794–807, May 1991.

[13] H. Hashemi, "The indoor radio propagation channel," *Proc. IEEE*, vol. 81, pp. 943–968, July 1993.

[14] T. S. Rappaport, *Wireless Communications: Principles and Practice*. Englewood Cliffs, NJ: Prentice-Hall, 1996.

[15] J. G. Proakis, *Digital Communications*, 3rd ed. New York: McGraw-Hill, 1995.

Andreas Springer (S'90–A'97) was born in Linz, Austria, in 1966. He received the Dipl.-Ing. degree in electrical engineering from the Technical University of Vienna, Vienna, Austria, in 1991, and the Dr.techn. (Ph.D.) degree from the University of Linz, Linz, Austria, in 1996.

From 1991 to 1996, he was with the Microelectronics Institute and, since 1997, he holds the position of an Assistant Professor at the Institute for Communications and Information Engineering, both at the University of Linz. He has been engaged in research work on GaAs integrated millimeter-wave TED's, monolithic microwave integrated circuits (MMIC's), and millimeter-wave sensor systems. His current research interests are focused on simulation of wireless communication systems in hostile environment, SAW-based spread-spectrum communication and indoor-radio channel modeling.

Dr. Springer is a member of the IEEE Microwave Theory and Techniques and IEEE Communications Societies.

Mario Huemer (S'98) was born in Wels, Austria, in 1970. He received the Dipl.-Ing. degree from the Johannes Kepler University of Linz, Linz, Austria, in 1996, and is currently working toward the Ph.D. degree in the field of wireless indoor communication systems.

In 1997, he joined the Institute for Communications and Information Engineering, Linz, Austria, where he is a Research and Teaching Assistant.

Leonhard Reindl (M'93) was born in Neuburg/Do, Germany, in 1954. He received the Dipl. Phys. degree from the Technical University of Munich, Munich, Germany, in 1985, and the Dr. Techn. degree from the University of Technology Vienna, Vienna, Austria, in 1997.

He is with Siemens AG Munich, Research and Development Center, Microacoustics Group, Munich, Germany, where he has been engaged in research and development on SAW convolvers, dispersive delay lines, tapped delay lines, ID tags, and wireless passive SAW sensors.

Clemens C. W. Ruppel (M'91–SM'92) was born in Munich, Germany, in 1952. He received the Diploma in mathematics from the Ludwig–Maximilians University of Munich, Munich, Germany, in 1978, and the Dr.techn. (Ph.D.) degree for work on the design of SAW filters from the Institut for Allgemeine Elektrotechnik and Elektronik of the Technical University of Vienna, Vienna, Austria, in 1986.

From 1984 to 1986, he was with the Corporate Research and Development Center, Microacoustics Group, Siemens AG Munich, Munich, Germany. From 1986 to 1990, he was the Assistant Manager for SAW filters and software development. In 1990, he became Group Manager and, in 1995, he became Project Manager. He has authored 40 papers (seven invited papers) on the design and simulation of SAW devices. His research interests include the design of bandpass filters, dispersive transducers, low-loss filters, and optimization algorithms.

Dr. Ruppel has been a member of the Technical Program Committee of the IEEE Ultrasonics Symposium since 1997, and voting member of the IEEE 802.11 Standards Committee.

Alfred Pohl (M'95), for photograph and biography, see this issue, p. 2212.

Franz Seifert (M'80–SM'86), for photograph and biography, see this issue, p. 2212.

Wolfgang Gugler (S'98) was born in Amstetten, Austria, in 1970. He received the Dipl.-Ing. degree from the Johannes Kepler University of Linz, Linz, Austria, in 1996, and where he is currently working toward the Ph.D. degree in the field of wireless SAW applications for high-data-rate communication systems.

In 1996, he joined the Institute for Communications and Information Engineering, Johannes Kepler University of Linz, where he is a Research and Teaching Assistant.

Robert Weigel (S'88–M'89–SM'95) was born in Ebermannstadt, Germany, in 1956. He received the Dr.-Ing. and Dr.-Ing.-habil. degrees in electrical engineering from the Technical University of Munich, Munich, Germany, in 1989 and 1992, respectively.

From 1982 to 1988, he was a Research Assistant, from 1988 to 1994, a Senior Research Engineer, and from 1994 to 1996, a Professor at the Technical University of Munich. In Winter 1994–1995, he was a Guest Professor at the Technical University of Vienna, Vienna, Austria. Since 1996, he has been Head of the Institute for Communication and Information Engineering, University of Linz, Linz, Austria. He has been engaged in research and development on microwave theory and techniques, integrated optics, high-temperature superconductivity, SAW technology, and digital and microwave communication systems. Within these fields, he has published over 120 papers and has given over 90 international presentations. His review work includes European research projects and international journals.

Dr. Weigel is a senior member of the IEEE Microwave Theory and Techniques and the IEEE Ultrasonics, Ferroelectrics, and Frequency Control Societies. He is also a member of the Institute for Systems and Components of The Electromagnetics Academy, the Informationstechnische Gesellschaft (ITG) in the Verband Deutscher Elektrotechniker (VDE), and the Society of Photo-Optical Instrumentation Engineers (SPIE). He was the co-recipient of the 1993 MIOP Award.